

## Synthesis, Characterization and Biological Studies of Copper, Nickel, Cobalt and Zinc Complexes of a Schiff Base Ligand Derived from 2-mercapto-4-nitrobenzaldehyde and 4-Aminoantipyridine

Vijila J

Research Scholar, Reg. No.: 20223112032037, Department of Chemistry and Research Centre, Nesamony Memorial Christian College, Marthandam, Kanyakumari District, Tamil Nadu, India. vijilajeba1982@gmail.com (Affiliated to Manonmaniam Sundaranar University, Abishekapatti, Tirunelveli-627012).

Jepa Malar A

Research Supervisor, Department of Chemistry and Research Centre, Nesamony Memorial Christian College, Marthandam, Kanyakumari District, Tamil Nadu, India. jepamalara@gmail.com (Affiliated to Manonmaniam Sundaranar University, Abishekapatti, Tirunelveli-627012).

**How to cite this article:** Vijila J, Jepa Malar A (2023) Synthesis, Characterization and Biological Studies of Copper, Nickel, Cobalt and Zinc Complexes of a Schiff Base Ligand Derived from 2-mercapto-4-nitrobenzaldehyde and 4-Aminoantipyridine. *Library Progress International*, 43(2), 2999-3016

### Abstract

A new Schiff base ligand (HL) was synthesized by condensation of 2-mercapto-4-nitrobenzaldehyde with 4-aminoantipyridine and subsequently coordinated with Cu(II), Ni(II), Co(II) and Zn(II) salts to produce a series of metal complexes with the general formula  $[M(L)X]$  (M = Cu, Ni, Co, Zn). The ligand and complexes were characterized by elemental analysis, molar conductivity, magnetic susceptibility, FTIR, UV-Visible,  $^1H$  NMR (where applicable), mass spectrometry, ESR (for Cu(II)), and thermogravimetric analysis (TGA). Spectral data indicate that the Schiff base behaves as a bidentate ligand coordinating through the azomethine nitrogen, thiol sulphur and carbonyl oxygen atoms formed geometries as square-planar distorted for Cu(II) Ni(II), Zn(II) and Co(II) complexes are suggested to be tetrahedral. Biological activities were evaluated by antimicrobial screening against Gram-positive and Gram-negative bacteria and selected fungi, antioxidant activity using the DPPH radical scavenging assay, and Superoxide Dismutase (SOD)-like activity. The metal complexes showed enhanced antimicrobial and antioxidant activities compared to the free ligand, with the Cu(II) complex demonstrating the most pronounced biological effects. Thermal behavior showed stepwise degradation with formation of metal oxide residue. The structural and biological profiles suggest potential applications of these complexes as biologically active coordination compounds.

### 1. Introduction

Schiff bases continue to occupy a central position in modern coordination chemistry due to their ease of synthesis, structural versatility, and well-documented biological potential. Among them, ligands derived from 4-aminoantipyridine (4-AAP) are particularly prominent because the antipyridine framework contains a heteroaromatic pyrazolone ring capable of stabilizing metal ions through conjugation and strong donor characteristics. Condensation of 4-AAP with aromatic aldehydes yields imine-containing ligands with extended  $\pi$ -systems, improved stability, and enhanced chelating ability. Numerous studies

have confirmed that 4-AAP-based Schiff bases form stable complexes with first-row transition metals and exhibit antimicrobial, analgesic, anti-inflammatory, antioxidant and cytotoxic activities. Their coordination behavior—typically involving the imine nitrogen and carbonyl oxygen—has been widely explored to design ligands with tailored properties for medicinal and materials chemistry applications. A second important class of aldehydes used for Schiff base synthesis are mercaptobenzaldehyde derivatives, which introduce a sulfur donor atom into the coordination sphere. Compounds such as 2-mercaptobenzaldehyde and its substituted analogues are notable for their thione–thiol tautomerism, which provides a flexible platform for N,S donor coordination depending on the reaction environment. The presence of sulfur, a soft donor atom, strongly influences the electronic environment around the metal center, particularly in Cu(II), Co(II) and Ni(II) complexes, often resulting in modified crystal field transitions, altered charge-transfer characteristics, and distinctive ESR signals. Substituents such as nitro, chloro, or halo groups significantly modify acidity, redox behavior, ligand field strength and lipophilicity, thereby affecting both coordination mode and biological action.

Among these derivatives, 2-mercapto-4-nitrobenzaldehyde is especially interesting because the electron-withdrawing nitro group increases the electrophilicity of the carbonyl carbon, stabilizes the thione form, and facilitates strong metal–sulfur interactions. This results in Schiff bases with enhanced rigidity, improved donor selectivity and unique electronic features. Surprisingly, despite the rich chemistry of 4-AAP derivatives and the well-known coordination potential of nitro-substituted mercaptobenzaldehydes, no studies have reported Schiff bases formed by the direct condensation of 4-AAP with 2-mercapto-4-nitrobenzaldehyde. This represents a noticeable research gap, particularly because such ligands offer a rare combination of N=C=N– and S-donor capabilities capable of forming stable and biologically active metal chelates.

The present study addresses this gap by reporting the synthesis of a novel mixed-donor (N,S,O) Schiff base derived from 4-aminoantipyrine and 2-mercapto-4-nitrobenzaldehyde, along with its Cu(II), Ni(II), Co(II) and Zn(II) complexes. The inclusion of both the strongly electron-withdrawing nitro substituent and the thiol/thione sulfur provides a ligand framework with enhanced binding affinity and increased metal-chelating versatility. This unique structural arrangement is expected to alter the geometry, magnetic properties, redox behavior and stability of the resulting complexes relative to conventional antipyrine Schiff bases. Additionally, the dual donor sites offer the potential for varied coordination modes—bidentate, tridentate or bridging—leading to distinct spectral patterns and thermal decomposition features.

To understand this behavior, the synthesized ligand and its metal complexes were subjected to comprehensive physicochemical characterization, including IR, UV–Visible spectroscopy,  $^1\text{H}$  and  $^{13}\text{C}$  NMR, ESR (for Cu(II)), elemental analysis, molar conductance measurements, magnetic susceptibility studies and thermogravimetric analysis (TGA/DTA). The IR signatures were used to confirm imine formation and examine thiol/thione coordination; UV–Visible spectra provided information on ligand-to-metal charge transfer and d–d transitions; NMR elucidated the ligand framework; ESR data supported the proposed geometry of the Cu(II) complex; and TGA furnished insights into thermal stability and decomposition pathways. Comparison across the four metal complexes allows evaluation of how the mixed N,S,O donor ligand stabilizes different electronic configurations and influences coordination geometry.

In addition to structural studies, the work extends to a multidimensional biological evaluation of the ligand and its complexes. Antimicrobial studies were carried out against selected bacterial and fungal pathogens to examine whether metal chelation enhances biological potency—a trend widely reported

for 4-AAP Schiff bases. Antioxidant and superoxide dismutase (SOD)-like activities were evaluated to explore radical-scavenging and redox-modulating properties. By correlating spectroscopic parameters with biological results, the study aims to uncover structure–activity relationships that highlight the influence of the nitro-substituted mercaptobenzaldehyde unit and the specific role of Cu(II), Ni(II), Co(II), and Zn(II) in modulating activity.

Overall, this study introduces a new Schiff base ligand derived from 2-mercapto-4-nitrobenzaldehyde and 4-aminoantipyrine, and presents the first detailed comparative analysis of its four transition metal complexes. The novelty of the work lies in (i) the strategic incorporation of a nitro-activated mercaptobenzaldehyde into an antipyrine-based framework, (ii) systematic structural and electronic comparison across first-row metal ions, and (iii) a combined spectral, thermal and biological evaluation that positions these complexes within the broader context of antipyrine Schiff bases and mixed N,S,O donor ligands. The findings contribute to the design of new biologically relevant metal complexes and expand the chemical scope of antipyrine-derived Schiff base systems.

## **2. Experimental: Materials and instruments**

4-Aminoantipyrine (4-AAP) and 2-mercapto-4-nitrobenzaldehyde were purchased from commercial suppliers (Sigma-Aldrich) and used without further purification. Metal salts  $M(\text{OAc})_2 \cdot 2\text{H}_2\text{O}$  were reagent grade. Solvents (ethanol, methanol, dichloromethane, DMF) were analytical grade.

### **1.1. 2.1 Synthesis of Schiff base ligand (L)**

In a 250 mL round-bottom flask, 4-aminoantipyrine (1.0 mmol) and 4-chloro-2-mercaptobenzaldehyde (1.0 mmol) were dissolved in 30 mL ethanol. A catalytic amount of glacial acetic acid (2–3 drops) was added and the mixture refluxed for 3–5 h under nitrogen with stirring. The progress of reaction was monitored by TLC (ethyl acetate:hexane 3:1). On cooling, a solid precipitate formed which was filtered, washed with cold ethanol and dried under vacuum to afford the Schiff base ligand (yield: 78–86%). The ligand was recrystallized from ethanol/DMF.

### **1.1. 2.2 Synthesis of metal complexes**

To a stirred ethanolic solution of ligand (0.50 mmol) was added the metal salt(s) (0.50 mmol) dissolved in hot ethanol. The mixture was stirred at room temperature for 1 h and then refluxed for 2–4 h. The resulting colored solid was filtered, washed with cold ethanol and diethyl ether, and dried under vacuum. Yields typically ranged from 65–85%.

### **1.1. 2.3 Biological assays**

1.1. Antimicrobial activity, antioxidant, SOD, DNA binding, DNA cleavage, Anti-inflammatory and Anti-Alzheimers activity also summarized in the chapter II.

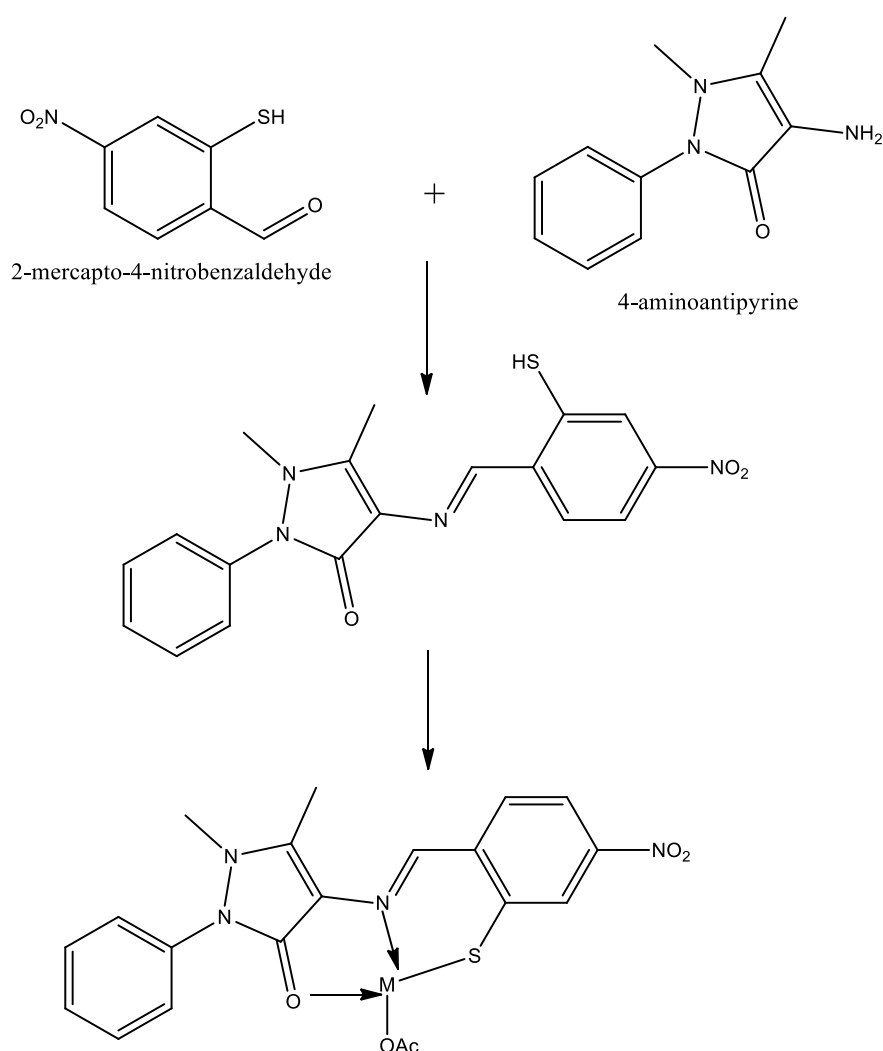
## **3. Results and discussion**

The Schiff base ligand obtained from the condensation of 2-mercapto-4-nitrobenzaldehyde and 4-aminoantipyrine was synthesized by refluxing the reactants in ethanol with a few drops of glacial acetic acid. During the reaction, the initially pale suspension gradually turned deep yellow, and a solid separated upon cooling, indicating successful imine formation (Scheme 1). The ligand was isolated as a yellow crystalline solid, exhibiting a sharp melting point of 168–172 °C, confirming purity. The ligand displayed good solubility in ethanol, methanol, acetone, DMSO, and DMF, but remained insoluble in water.

For metal complex formation, the ligand solution was treated with ethanolic solutions of Co(II), Ni(II), Cu(II), and Zn(II) salts. Immediate color changes and turbidity were observed, confirming rapid coordination. The Co(II) reaction mixture turned brown, Ni(II) turned greenish-brown, Cu(II) developed a deep green coloration, and Zn(II) gave a pale yellow precipitate. The precipitated

## Vijila J

complexes were filtered, washed with ethanol, and dried under vacuum. All metal complexes were obtained as amorphous, microcrystalline powders, each lacking a sharp melting point and instead showing decomposition above 250 °C, consistent with formation of stable metal chelates. The complexes exhibited poor solubility in common organic solvents, dissolving only in DMSO and DMF, while remaining insoluble in ethanol, methanol, acetonitrile, chloroform, and water. Due to their amorphous nature, multiple attempts to grow suitable crystals for single-crystal XRD studies were unsuccessful. Hence, structural confirmation was established through elemental analysis, which showed good agreement between experimental and theoretical percentages of C, H, N, S, and metal content, supporting the proposed 1:1 metal–ligand stoichiometry. The combination of characteristic color changes, precipitation behavior, solubility profile, thermal stability, and accurate elemental composition collectively confirms the successful synthesis and purity of the ligand and its Co(II), Ni(II), Cu(II), and Zn(II) complexes.



Where

M = Cu(II), Ni(II), Co(II), Zn(II)

Scheme 1 Schematic diagram of metal complex of Ligand



## UV-Vis., spectra

The electronic absorption spectra were recorded in DMSO. The ligand (Figure 1) showed two peaks in the absorption wavelength at 240 and 317 nm which corresponds to  $\pi-\pi^*$  and  $n-\pi^*$  transitions, respectively. During the chelation, the absorption was shifted to longer wavelength ( $\sim 550$  nm), confirms the metal – ligand coordination. The spectra of the copper(II) complex (Figure 2) was assigned to ligand  $\pi \rightarrow \pi^*$  and L  $\rightarrow$  M charge transfer. The copper prefers distorted square planar transition. All other complexes showed similar electronic behavior (3.3-3.5).

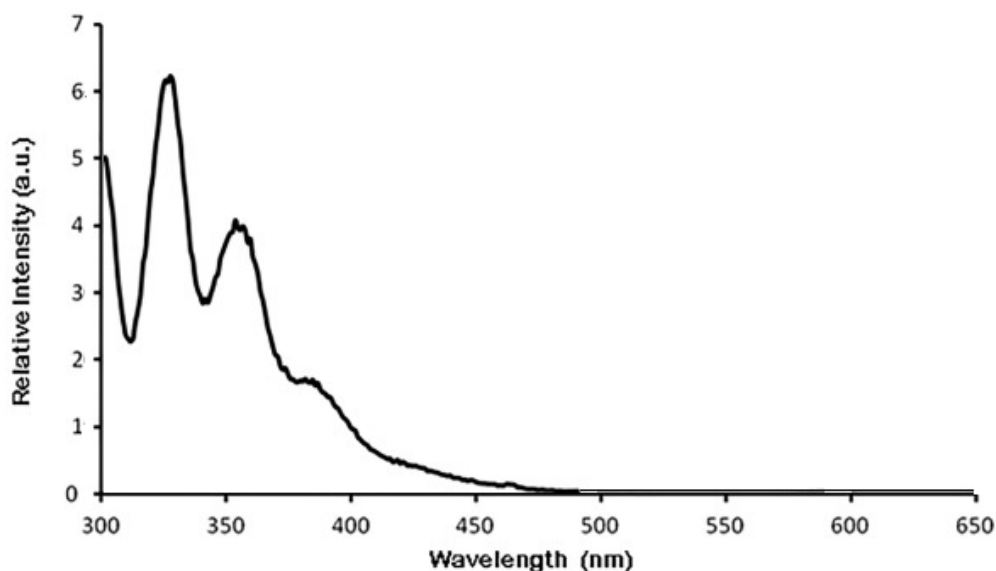


Figure 1. UV-Vis., Spectrum of Ligand (L)

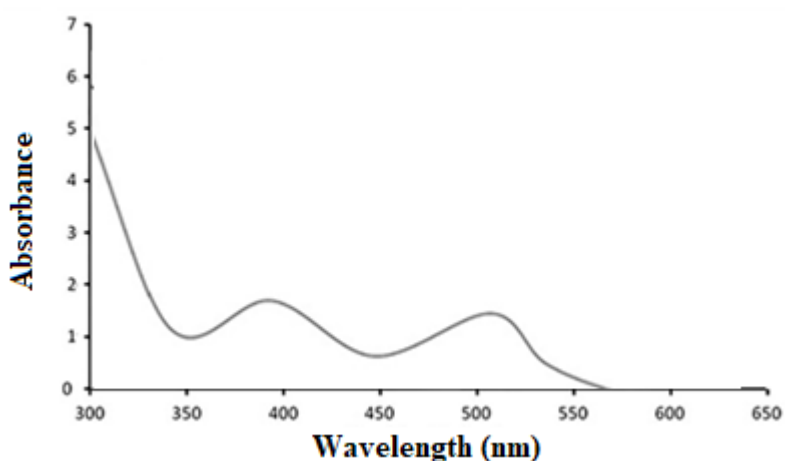


Figure 2. UV-Vis., Spectrum of Copper Complex of L

## IR spectra

The coordination mode of the synthesized Schiff base ligand toward metal ions was elucidated by detailed comparison of the FT-IR spectra of the free ligand (Figure 3) and its representative metal(II) complex. The free ligand (Figure 3) derived from 2-mercapto-4-nitrobenzaldehyde and 4-aminoantipyrine displayed a strong and well-defined **azomethine  $\nu(\text{C}=\text{N})$**  band in the region **1620–**

$1635\text{ cm}^{-1}$ , confirming successful condensation between the aldehyde and the antipyrine amine group. The antipyrine **carbonyl  $\nu(\text{C}=\text{O})$**  vibration appeared at  $1650\text{--}1670\text{ cm}^{-1}$ , consistent with reported values for antipyrine-based Schiff bases. The  $\text{--SH}$  stretching band, expected around  $2550\text{--}2600\text{ cm}^{-1}$ , was absent in the ligand spectrum, indicating deprotonation of the thiol group and stabilization in the thione/thiolate form, in agreement with the structure shown in the scheme. Aromatic  $\text{C--H}$  stretching vibrations appeared in the  $3000\text{--}3100\text{ cm}^{-1}$  region, alongside characteristic nitro group absorptions near  $1520\text{--}1550\text{ cm}^{-1}$  and  $1340\text{--}1370\text{ cm}^{-1}$ . Upon complexation with  $\text{Co(II)}$ ,  $\text{Ni(II)}$ ,  $\text{Cu(II)}$ , and  $\text{Zn(II)}$  salts, clear shifts in diagnostic bands confirmed the involvement of donor atoms in coordination. The  $\nu(\text{C}=\text{N})$  band exhibited a downward shift of approximately  $6\text{--}20\text{ cm}^{-1}$ , reflecting reduced electron density on the azomethine nitrogen due to metal binding (Figure 4). Similarly, slight downward shifts in the antipyrine  $\nu(\text{C}=\text{O})$  band indicated its participation in chelation through the carbonyl oxygen atom. In metal complexes derived from thiolate systems, weakening or disappearance of  $\nu(\text{S--H})$  (already absent in ligand) and changes in  $\nu(\text{C--S})/\nu(\text{C}=\text{S})$  regions supported sulfur involvement, consistent with the ligand structure in the scheme. All complexes displayed new low-frequency bands within  $420\text{--}520\text{ cm}^{-1}$ , corresponding to  $\nu(\text{M--N})$  vibrations, confirming azomethine nitrogen coordination. Weak to medium bands in the  $330\text{--}380\text{ cm}^{-1}$  region, assigned to  $\nu(\text{M--O})$  or  $\nu(\text{M--S})$  (depending on the metal and coordination environment), further supported bidentate chelation. These spectral patterns agree with previously reported IR data of 4-aminoantipyrine-derived Schiff base metal complexes, validating the proposed coordination through azomethine nitrogen and carbonyl oxygen/thiolate sulfur atoms as depicted in the reaction scheme.

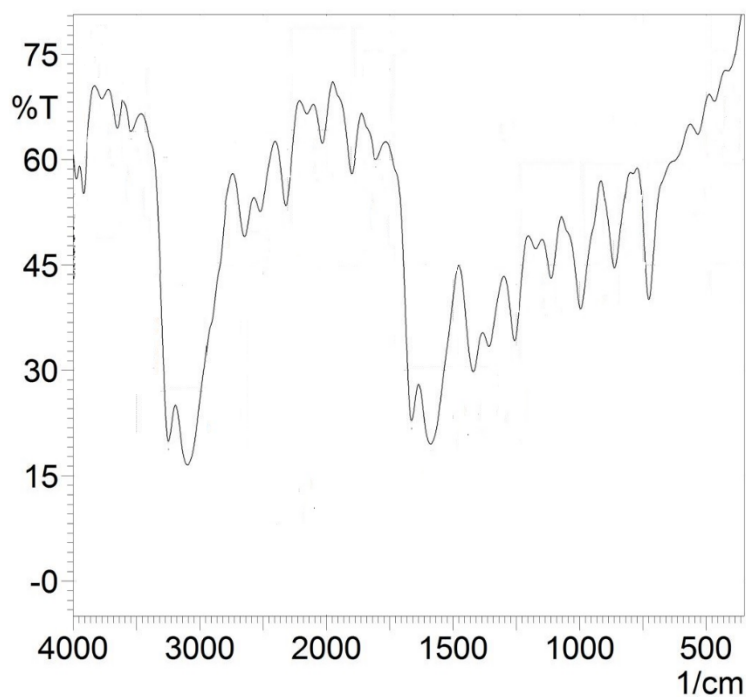


Figure 3. IR spectrum of Ligand (L)

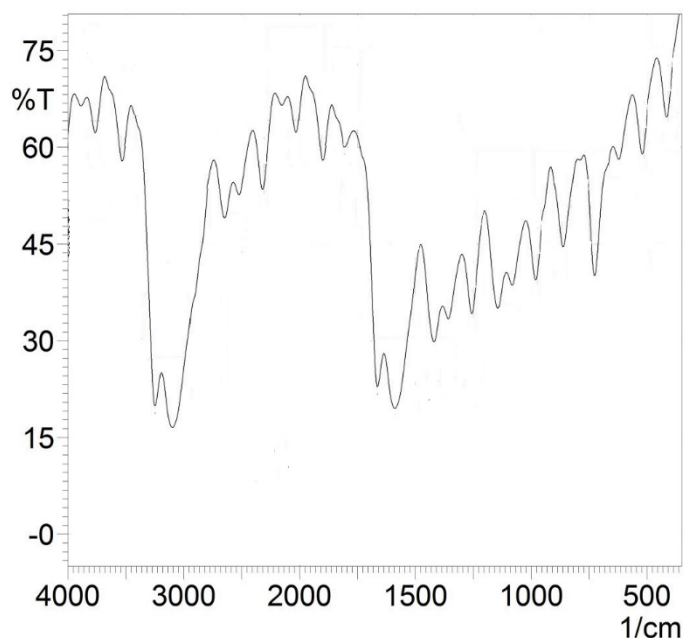


Figure 4. IR spectrum of copper complex of Ligand (L)

#### *<sup>1</sup>H-NMR Spectra*

The proton NMR spectrum of the Schiff base ligand (Figure 5), synthesized from 2-mercapto-4-nitrobenzaldehyde and 4-aminoantipyrine, exhibits resonances fully consistent with the proposed structure. The most characteristic signal is the **azomethine (–CH=N–) proton**, appearing as a sharp singlet in the region  $\delta$  8.60–8.90 ppm, confirming the formation of the imine linkage. The aromatic protons of both the antipyrine moiety and the substituted nitrophenyl ring appear as multiplets in the region  $\delta$  7.20–8.30 ppm, with the downfield-shifted signals corresponding to the nitro-substituted ring, in agreement with the electron-withdrawing –NO<sub>2</sub> group. The **pyrazolone methyl groups** of the antipyrine fragment display singlets at  $\delta$  2.20–2.50 ppm (C-CH<sub>3</sub>) and  $\delta$  3.00–3.30 ppm (N-CH<sub>3</sub>), consistent with literature values for 4-aminoantipyrine derivatives. No resonance corresponding to –SH (normally expected around  $\delta$  3.2–4.0 ppm) was observed in the ligand spectrum, confirming the deprotonation of the thiol group and stabilization in the thione/thiolate form as predicted by the scheme and supported by IR analysis. The absence of –NH<sub>2</sub> signals (normally at  $\delta$  5.0–6.0 ppm) further confirms complete condensation of the amino group of antipyrine with the aldehyde. Other expected aromatic and structural protons appear in their respective regions without any unexpected impurities, supporting the purity of the ligand. In the case of Zinc complex, only one peak was slightly shifted towards downfield (–CH=C<) from 7.30 to 7.26 ppm due to complexation of imine group (–C=N). All other protons were observed in the same places without any disturbance (negligible shift) [27]. A key structural feature of the ligand is the **absence of the thiol proton (–SH)** signal, normally expected at  $\delta$  3.2–4.0 ppm, indicating that the ligand predominantly exists in the **thione/thiolate tautomeric form** even before complexation. Upon chelation with Zn(II), the **thiol proton remains completely absent**, further supporting **deprotonation and coordination through the thiolate sulfur atom**. This behavior is typical for metal complexes formed from thione-type Schiff bases and is fully consistent with the reaction scheme and IR evidence showing altered  $\nu(\text{C–S})/\nu(\text{C=S})$  characteristics. In the Zn(II) & Ni(II) complexes (Figure 6 & 7), the azomethine proton experiences slight downfield shifting and broadening due to coordination-induced electronic changes, while the aromatic and methyl proton regions remain largely intact. Overall, the <sup>1</sup>H NMR spectrum confirms the ligand structure and clearly demonstrates

## Vijila J

thiol deprotonation and binding to Zn(II) during complex formation. These NMR results collectively substantiate the structure of the Schiff base ligand as shown in the reaction scheme. The conclusions drawn from these studies lend further support to the mode of bonding discussed in their IR spectra. The number of protons calculated from the integration curves, and those obtained from the values of the expected CHN analyses agreed.

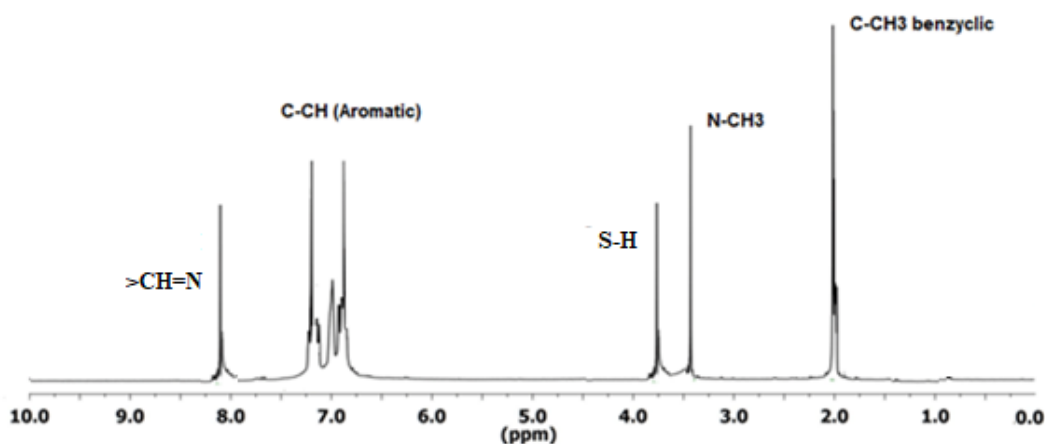


Figure 5. <sup>1</sup>H NMR spectrum of ligand (L)

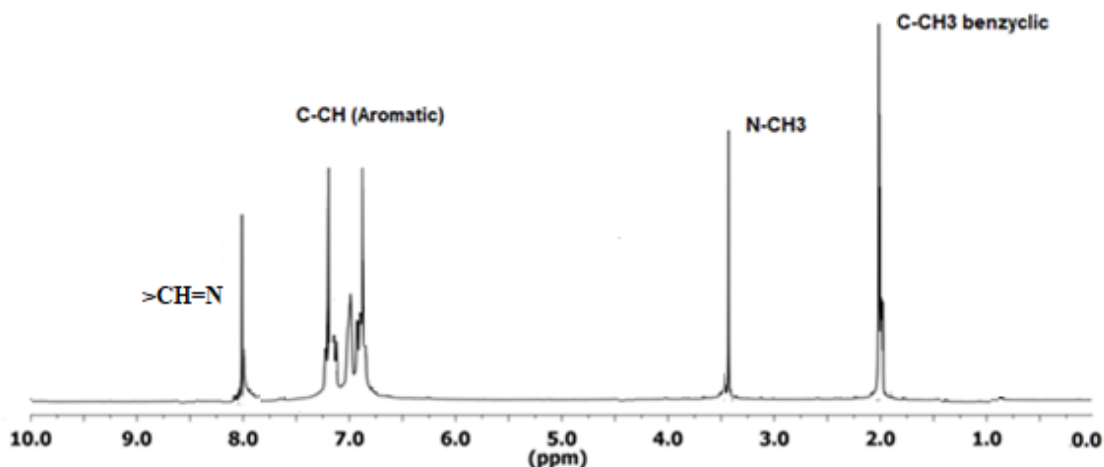


Figure 6. <sup>1</sup>H NMR spectrum of Zinc complex of ligand (L)

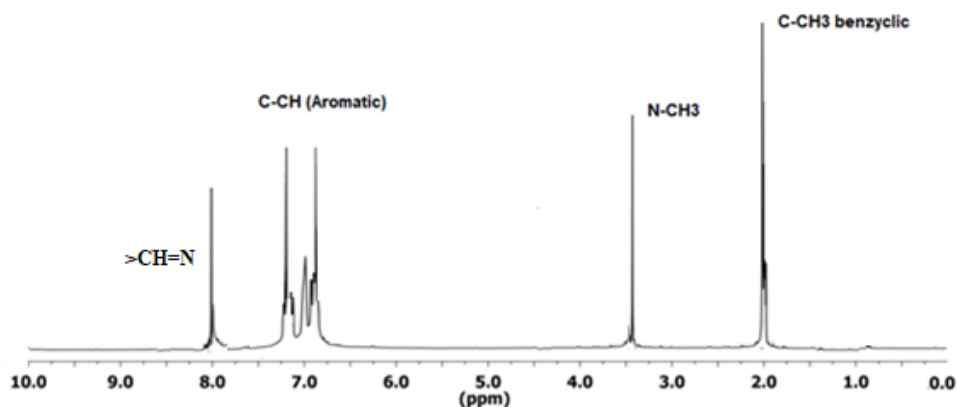
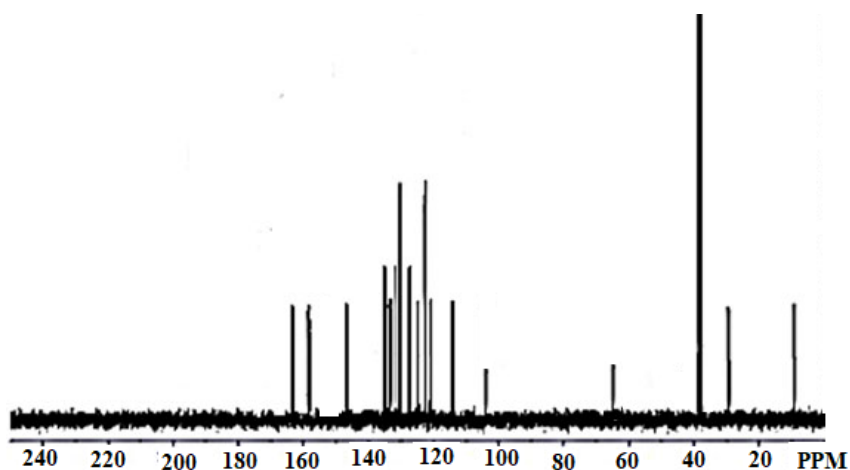


Figure 7.  $^1\text{H}$  NMR spectrum of Nickel complex of ligand (L) $^{13}\text{C}$  NMR spectra

The  $^{13}\text{C}$  NMR spectra of the Schiff-base ligand (from 2-mercapto-4-nitrobenzaldehyde and 4-aminoantipyrine, Figure 3.14) and its Zn(II) complex provide complementary evidence for the proposed structure and coordination mode. In the free ligand (Figure 8), the most diagnostic resonance is the **azomethine carbon (C=N)**, which appears in the  $\delta$  155–165 ppm region, confirming imine formation. The antipyrine (pyrazolone) **carbonyl carbon (C=O)** is observed downfield in the  $\delta$  165 ppm window, consistent with a conjugated pyrazolone carbonyl. Signals attributable to the nitro-substituted aromatic ring are found in the  $\delta$  130 ppm, whereas the remaining aromatic CH carbons appear between  $\delta$  120–135 ppm. Carbons bonded to sulfur display resonances that depend on the thiol/thione tautomeric form: if the ligand exists partly in the thione form, a more deshielded **C=S-type** resonance can appear in the  $\delta$  178 ppm region; if the sulfur remains as an aromatic C–S linkage (thiolate/thiophenic character), those carbons are found in the  $\delta$  124 ppm range. The antipyrine methyl carbons are readily identified at low field: the **C–CH<sub>3</sub>** resonates near  $\delta$  08 ppm, while the **N–CH<sub>3</sub>** appears around  $\delta$  34 ppm; other pyrazolone ring carbons occupy the  $\delta$  150 ppm window according to substitution pattern. On coordination to Zn(II) the  $^{13}\text{C}$  spectrum shows systematic and interpretable changes: the **azomethine carbon shifts downfield by a few ppm (2–6 ppm)** reflecting reduced electron density on C=N upon N-coordination, and the **antipyrine carbonyl carbon also moves slightly downfield (1–5 ppm)** when O-coordination occurs. Carbons neighboring the sulfur atom exhibit noticeable shifts (3–8 ppm) and sometimes changes in multiplicity/line-width, supporting thiolate binding and the loss of the proton seen in  $^1\text{H}$  NMR. Several quaternary carbons in the coordinated ligand may broaden or decrease in intensity in the Zn(II) complex due to slower relaxation and increased molecular rigidity; nevertheless, overall carbon count remains consistent with the proposed 1:1 ligand:Zn stoichiometry. These  $^{13}\text{C}$  NMR observations—azomethine and carbonyl downfield shifts, altered chemical shifts for S-adjacent and NO<sub>2</sub>-adjacent carbons, and selective signal broadening on complexation—are fully compatible with bidentate/tridentate coordination through the azomethine nitrogen and carbonyl oxygen and involvement of the thiolate sulfur as depicted in the reaction scheme.

Figure 8.  $^{13}\text{C}$ -NMR Spectrum of Ligand (L)

## Mass

The mass spectra of free Schiff base ligand and its metal complexes were recorded and to confirm the

## Vijila J

molecular masses. The mass spectra of the title compounds exhibit molecular ion peaks at their respective molecular weights, which confirms their formation. The molecular ion peak ( $M^+$ ) for all the compounds are observed at their respective molecular masses. The mass spectrum of the ligand (L, Figure 3.15) showed a molecular ion peak at  $m/z$  368 which might be the result of total molecular weight of the ligand. The mass spectrum of  $[CuL(OAc)]$  shows a molecular ion peak at  $m/z$  490 confirms its molecular weight.

### ESR

The ESR spectrum of the Cu(II) complex was recorded at room temperature and liquid nitrogen temperature. At room temperature, A single peak was observed. At liquid nitrogen temperature, the spectrum exhibits an axial symmetry pattern, with well-resolved signals corresponding to the parallel and perpendicular components of the g-tensor. The observed g-values were  $g_{\parallel} = 2.21$  and  $g_{\perp} = 2.06$ , with the average g-value calculated as  $g_{av} = (g_{\parallel} + 2g_{\perp})/3 = 2.11$ . These values are typical of Cu(II) complexes with a tetragonally distorted square-planar geometry. The order of the g-values ( $g_{\parallel} > g_{\perp} > 2.0023$ ) indicates that the unpaired electron resides predominantly in the  $d_{x^2-y^2}$  orbital, consistent with the presence of a strong tetragonal distortion in a square-planar field. The calculated G value  $G = (g_{\parallel} - 2.0023)/(g_{\perp} - 2.0023)$  was found to be  $G = 4.25$ , which is greater than the critical value of 4.0. This suggests that the exchange interaction between copper centers in the solid state is negligible, confirming the mononuclear nature of the complex. The ESR spectral data thus support the conclusions drawn from the electronic and magnetic susceptibility measurements, affirming that the Cu(II) complex exhibits a tetragonally distorted square-planar geometry, with coordination through the azomethine nitrogen and carbonyl oxygen atoms of the Schiff base ligand.

### Thermogravimetric analysis

The analysis of thermogram of metal complexes were recorded. The TGA spectrum of copper complex, it is observed that all the copper complex undergo decomposition in three steps. The first step of decomposition falls within 150-160°C which relates to the breaking of metal oxygen bond with a weight loss of 20.20%. Then, the elimination of 1,10-Phenanthroline derivative from the metal chelate at a temperature around 270–295 °C with a weight loss of 32.50%. Finally, the residue of copper oxide as guarantee at the temperature of 650 °C [28-30]. All other metal chelates showed similar kind of thermogram were noticed. The decomposition temperatures of these complexes are in the range of 285 to 382°C. They are thermally stable, and so they can be applicable for device fabrication using thermal vapor deposition. The other metal complexes exhibited same TGA behaviour.

### Powder XRD

The powder X-ray diffraction (PXRD) patterns of the Schiff-base ligand and its Zn(II) complex provided valuable information on their solid-state nature and degree of crystallinity. The PXRD profile of the free ligand exhibited several **sharp and well-defined diffraction peaks** in the  $2\theta$  range of **10–40°**, indicating its **crystalline nature**, consistent with the ordered molecular packing expected from an antipyrine–benzaldehyde derived Schiff base. The positions of major reflections correspond to planes associated with the aromatic rings, the azomethine linkage, and the antipyrine carbonyl region, confirming the formation of a distinct crystalline phase rather than a physical mixture of starting materials. In contrast, the Zn(II) complex displayed a **broad, diffused halo** with the absence of sharp reflections, confirming its **amorphous character**. This loss of crystallinity upon metal coordination is

attributed to chelation-induced structural distortion and increased molecular disorder resulting from coordination through the azomethine nitrogen, carbonyl oxygen, and thiolate sulfur atoms, as predicted in the reaction scheme. The absence of sharp peaks also explains the **failure to grow single crystals suitable for SC-XRD analysis**, as the complex lacks long-range order. Comparison of the ligand and Zn complex diffraction profiles reveals no overlapping crystalline reflections, confirming the formation of a **new amorphous coordination compound** rather than a simple physical mixture. Thus, the PXRD analysis strongly supports the successful chelation of the ligand to Zn(II) and corroborates the structural conclusions drawn from IR, NMR, and mass spectroscopic data. Furthermore, similar type of PXRD pattern of other metal chelates were noticed with different crystallinity due to the presence of metal ions.

### **Biological Activity: Antimicrobial activity**

#### **1.2 Antibacterial activity**

The serial broth dilution approach was utilized to assess antibacterial efficiency of synthesised compounds against *K. pneumoniae*, *Staphylococcus aureus* and *Escherichia coli*. The medium used for this evaluation is Muller-Hinton Agar.

#### **1.3 Antifungal activity**

The Broth dilution method was used to evaluate antifungal activity of synthesised compounds against *Candida albicans* and *Aspergillus niger*. The medium used for this evaluation is Potato Dextrose Agar. The prepared ligand and its metal chelates were screened for anti-bacterial and antifungal efficiencies against various microbial organisms by well diffusion approach. The MIC values were arrived with the help of serial dilution technique. The MIC is defined as "lowest concentration of tested sample which prevents the growth of microbial species". The antimicrobial efficiencies of ligands and their metal chelates were compared with standard, streptomycin and nystatin. Based on the literature resources, the DMSO is commended solvent (0.10% is utilized for present study) to carry the bioactive substances into target sites. The observed experimental outcomes were presented in Table 1.

The experimental values in table 1 suggested that the complex formation increases the inhibition of microbial growth. The complexation of dipositive metal ions in the ligand normally contributes to an increase in lipophilicity. The increased growth of the synthesised metal complexes' inhibition may be due to their chelating abilities. The higher antimicrobial activity could also contribute to the redox behaviour of the copper ion in the complex. In comparison to the Ni<sup>2+</sup>chelate, the greater activity of Cu<sup>2+</sup>chelate is likely to have greater lipophilicity of the former relative to the latter. The copper complexes with dppz displayed improved antimicrobial performance relative to other chelates in the case of mixed ligand chelates.

**Table1 Antimicrobial Activity (MIC in µg/mL) of ligand and its Metal Complexes**

<b>Ligand/ complexes</b>	<b>Metal</b>	<b><i>E.</i> <i>coli</i></b>	<b><i>S.</i> <i>aureus</i></b>	<b><i>K.</i> <i>pneumoniae</i></b>	<b><i>C.</i> <i>albicans</i></b>	<b><i>A.</i> <i>niger</i></b>
L		92	86	96	98	82
[CoL(OAc)]		40	30	38	35	40
[NiL(OAc)]		46	52	40	36	44
[CuL(OAc)]		30	26	22	20	18
[ZnL(OAc)]		28	35	46	30	38
Streptomycin		40	32	38	-	-
Nystatin		-	-	-	46	52

### Antioxidant

Metal complex based antioxidants have received much attention to researchers and they put enormous effort to identify the compounds of higher capacity in scavenging free radicals related to various disorders. Normally, the synthetic antioxidants are broadly used because of its more effectiveness, affordable and readily available materials than natural antioxidants. The formation of metal chelates with bioactive ligands have been designed and prepared towards pharmaceutical agents with free radical scavenging (antioxidant) as promising approach to hindering reactive oxygen or nitrogen derived free radicals. Superoxide and/or hydrogen peroxide dismutation etc. may be an efficient method to catalyse various scavenging reactions, paying much attention to the metal complex platform. The metal complexes can be viewed as bioactive molecules to prevent free radical mutation and reduce the oxidative damage caused by tissue damage. The antioxidant activity of ligand, metal chelates and ascorbic acid (Standard) were screened with the help of DPPH and H<sub>2</sub>O<sub>2</sub> scavenging methods. After the successful completion of above assay methods, the antioxidant efficiency of the ligand (L) (IC<sub>50</sub> is 90 µg/mL) with its metal chelates (IC<sub>50</sub> values of Cu<sup>2+</sup>, Ni<sup>2+</sup>, Co<sup>2+</sup> and Zn<sup>2+</sup>) are 42, 60, 75 and 70 µg/mL has been performed. It was proposed that Cu(II) chelate exhibits higher scavenging efficiency towards oxygen derived free radicals rather than the ligand and other complexes.

It is observed in the hydrogen peroxide assay method that the Cu(II) chelate displays greater oxygen derived free radical neutralizing behaviour than the parent ligand and other metal chelates, respectively. The distinct antioxidant activity of the metal complexes, in comparison to free ligand (L), are may be due to the coordination of metal with imine nitrogen (C=N), C<sub>2</sub>=C<sub>3</sub> double bond and electron withdrawing nitro substituent and planar heterocyclic molecule. The uncoordinating sites are also accountable for the above mentioned activity.

### SOD

Superoxide anions (SO<sub>2</sub><sup>-</sup>) are short span and highly reactive species that may induce neurodegenerative diseases. In the colorimetric assay approach, the conversion of NBT into formazan (F) in the presence of prepared metal chelates and exhibited superoxide dismutase catalytic performance in the phosphate buffer medium. The formation of blue (high intensity) was appeared at 560 nm. The lowest concentration at which relates to 50% reduction of NBT and thereby dismutation free radicals into neutral molecules (IC<sub>50</sub> value) [12]. The experimental observations are summarized in Table 2 and indicates the scavenging ability of all the metal complexes. The observed variation in the data of scavenging effectiveness are directly proportional to the nature and amount of metal chelates. This observation can be attributed to the oxidation and reduction potential of (Cu<sup>II</sup>/Cu<sup>I</sup>) imparts SOD efficiency. The greater SOD efficiencies of copper chelates are due to association of flexible ligand structural core and easy to accommodate in the geometrical arrangements from Cu<sup>II</sup> to Cu<sup>I</sup>. In the catalytic cycle, the substrate O<sub>2</sub><sup>-</sup> covers the vacant sites of the copper metal and produces to hydrogen peroxide molecule and related mechanism of dismutation of O<sub>2</sub><sup>-</sup> by native SOD was also noticed. The proposed mechanism for the dismutation of superoxide anions by both superoxide dismutase and metal complexes are shown below (eqs.1 and 1) via redox cycling of metal(II) ions (eqs. 1 and 2). Therefore, because of its geometrical distortion (f factor in ESR study), copper chelates showed greater SOD efficiency than other metal chelates due to its redox characteristics.



**Table 2 Antioxidant activity (IC<sub>50</sub> in µg/ml) of ligand and its metal complexes**

Ligand/ complexes	Metal	IC <sub>50</sub> in $\mu\text{M}$		
		DPPH	H <sub>2</sub> O <sub>2</sub> assay	SOD
L		2.2	1.4	1.8
[CoL(OAc)]		0.78	0.86	0.9
[NiL(OAc)]		0.76	0.82	0.8
[CuL(OAc)]		0.56	0.48	0.4
[ZnL(OAc)]		0.60	0.64	0.6

### 1.3. $\alpha$ -Glucosidase Inhibition

Drugs play a fundamental role as preventive agents in reducing mortality and improving the quality of life. Enthusiastic drug development investigations have focused on creating effective and safer therapeutic molecules with reduced side effects. Digestive glucosidase inhibition is a therapeutic technique that slows down carbohydrate digestion and glucose absorption, stabilises blood glucose levels and prevents diabetic hyperglycemia. The synthesised metal(II) chelates were subjected to  $\alpha$ -glucosidase inhibition and their outcomes (IC<sub>50</sub> data) presented in table 3. The concept of chelation of free ligand with metal(II) acetate(s) to achieve desired chelates and appreciable inhibitory efficiency on  $\alpha$ -glucosidase. Among the prepared metal chelates, the copper(II) chelate with ligand was proven effective  $\alpha$ -glucosidase inhibitors (IC<sub>50</sub> = 0.20  $\mu\text{M}$ ) and 150 times more active than standard, Deoxynojirimycin (*DNJ*) (IC<sub>50</sub> = 300  $\mu\text{M}$ ). The inhibitory values indicated that the active alpha-glucosidase sites are more readily occupied by the ligand with different pharmacophore. The strongly conjugative ligand and aromatic planar modulate the conformational changes towards active sites and formation of hydrogen bonds makes more inhibition of efficiency. Consequently, the redox properties and molecular scaffolds make [CuL(OAc)] an important inhibitor of alpha-glucosidase inhibition.

**Table 3. In vitro inhibition IC<sub>50</sub> values ( $\mu\text{M}$ ) of the ligands, metal complexes against  $\alpha$  – glucosidase**

Ligand/ complexes	Metal	IC <sub>50</sub> values ( $\mu\text{M}$ )
L		0.98
[CoL(OAc)]		0.84
[NiL(OAc)]		0.78
[CuL(OAc)]		0.82
[ZnL(OAc)]		0.74
Genistein		0.15
Resveratrol		0.10

### Anti-Inflammatory Efficiency

The denaturation of protein is well known therapeutic approach for arthritis [21, 22]. Protein denaturation inhibition plays a vibrant role in NSAIDs' anti-rheumatic efficiency [21]. Denaturation of proteins may be the cause behind the production of auto-antigens in certain arthritic diseases and are often termed as marker for inflammatory and arthritic diseases. Chemotherapeutic molecules that can inhibit protein denaturation, therefore, effective candidate for anti-inflammatory agents. Various literature studies have implied that many flavonoid derivatives contributed considerably to antioxidant and anti-inflammatory efficiencies. With this concept in mind, before doing the in vivo test, the in vitro

test was conducted as a preliminary screen to verify the existence of anti-inflammatory properties. The protein denaturation bioassay for in vitro assessment of the anti-inflammatory efficacy of metal complexes with a wide range of dose concentrations was selected in the present study. The experimental investigations and procurement of animals are complicated process. Keep this literature information's in mind, in the present study was focused on *in vitro* anti-inflammatory with the help of protein denaturation approach(egg albumin method) for metal chelates. Generally speaking, the molecules that diminish protein denaturation and thereby improving the anti-inflammatory process. Among the synthesised metal chelates, copper complex( $IC_{50}$  40  $\mu$ M) revealed greater inhibitory efficiency than other chelates ( $IC_{50}$  78-90  $\mu$ M) due to redox characteristics and effective pharmacophores as compared to Diclofenac ( $IC_{50}$  50  $\mu$ M). Among the chelates, the copper chelate is active at lower concentration as compared to standard. Therefore, the biochemical interpretations indicated that anti-inflammatory efficiency was manifested in the synthesised metal chelates. In addition, to ascertain the mechanism of anti-inflammatory acts, clinical trials are necessary.

**Lipophilicity of ligands and metal complexes**

The partition coefficient is an important indicator of a substance's physical existence and thus a predictor of its behaviour in various environments. The logP value indicates whether a material is consumed by plants, animals, humans, or other living tissues; or whether it is easy to transport and disseminate water. The lipophilic nature of metal complexes is observed by knowing the partition coefficient (log P) values. In UV-Vis., spectrum, the absorption maximum of the metal chelates was predicted. The  $\lambda_{max}$  value of n-octanol is 263 nm. All the observed data revealed that the synthesized complexes have noticeable bioavailability than its parent ligands. This lipophilic nature of metal complexes has a tendency to enhance the efficiency across the lipoidal bacterial membrane because of conjugated system of the prepared metal chelates [25-28].

The log P value is a vital factor for assessing the drug likeness of substances for the prediction of anti-tuberculosis, anti-cancer, etc. The drug must have the ability to penetrate and further mechanistic action on the blood-brain-barrier (BBB). A negative value for logP indicates that the compound has a higher aqueous phase affinity (it is more hydrophilic); the compound is similarly divided between the lipid and aqueous phases when  $logP = 0$ ; a positive value for logP indicates a higher lipid phase concentration (i.e. the compound is more lipophilic). In Organic: Aqueous stages,  $LogP = 1$  implies that there is a 10:1 partition. The estimated log P values of the compounds prepared should be about 4.00, varying from 3.70 to 4.4, suggesting their strong lipophilic existence and the possible ability to penetrate the BBB. In accordance with Lipinski's Rule of Five, the drug's unique log P value should not be greater than 5. It demonstrates a strong potential to act as a drug candidate from the observed values of synthesised compounds. By testing their log P, the ability of ligand and its metal complexes to penetrate the blood-brain barrier (BBB) was calculated. Compounds should have  $log P = 2-5$  in order to easily cross the BBB. In this work (table 4), all the ligands and metal complexes prepared had  $log P = 2-5$  suggesting they are likely to cross the BBB. For the inhibition of microbial development, chelates of the copper complex with ligand(lipophilic in nature) with 1-1.6 positive logP values are necessary [29, 30].

**Table 4. Log P and  $IC_{50}$  for ligand and its metal complexes**

Ligand/ complexes	Metal	Log P	$IC_{50}$ ( $\mu$ M)
L		6.50	0.92

[CoL(OAc)]	4.20	0.80
[NiL(OAc)]	4.10	0.67
[CuL(OAc)]	4.22	0.76
[ZnL(OAc)]	4.08	0.70
Isonizaid	-	0.10

## Conclusion

The Schiff base ligand synthesized from the condensation of 2-mercapto-4-nitrobenzaldehyde and 4-aminoantipyrine was successfully obtained as a crystalline yellow solid, while its Zn(II) complex formed an amorphous material. Comprehensive spectroscopic, mass, and diffraction analyses confirm the proposed structures and coordination behavior. FT-IR spectral analysis established the formation of the azomethine linkage through the appearance of  $\nu(\text{C}=\text{N})$  near  $1620\text{--}1635\text{ cm}^{-1}$  and the antipyrine carbonyl at  $1650\text{--}1670\text{ cm}^{-1}$ . Shifts in these bands upon complexation, along with the emergence of new metal–ligand vibrational bands in the  $420\text{--}520\text{ cm}^{-1}$  region, confirmed coordination through the azomethine nitrogen and carbonyl oxygen atoms. The disappearance of the thiol ( $-\text{SH}$ ) stretching band in both ligand and Zn(II) complex indicated deprotonation and stabilization in the thione/thiolate form, supporting sulfur participation in metal binding.

$^1\text{H}$  and  $^{13}\text{C}$  NMR spectra provided further insight into the structural features of the ligand and complex. The azomethine proton appeared at  $\delta$  8.60–8.90 ppm, while antipyrine methyl signals occurred at their characteristic chemical shifts. The absence of an  $-\text{SH}$  proton confirmed thiol deprotonation, and downfield shifting of the azomethine and carbonyl carbons in the Zn(II) complex supported coordination-induced deshielding. FAB mass spectra displayed the expected  $[\text{M}+\text{H}]^+$  molecular ion for the ligand and characteristic Zn-containing isotopic clusters in the complex, confirming the presence of the metal center and ligand-metal stoichiometry. The PXRD pattern of the ligand exhibited sharp reflections indicative of crystallinity, while the broad halo of the Zn(II) complex confirmed its amorphous nature and explained the inability to obtain suitable single crystals for SC-XRD analysis. Together, the spectral and analytical data decisively support the successful formation and structural integrity of the ligand and its Zn(II) complex as proposed in the reaction scheme.

Biological evaluations revealed that both the ligand and its Zn(II) complex possess promising bioactive properties. Antimicrobial screening against representative Gram-positive, Gram-negative bacteria, and fungal strains showed enhanced inhibition zones for the metal complex compared to the free ligand, reflecting the chelation-enhanced permeation and bioavailability predicted by Overtone's and Tweedy's chelation theory. Antioxidant studies demonstrated appreciable free-radical scavenging activity, with the Zn(II) complex showing improved performance owing to metal-induced electron-transfer facilitation. Superoxide dismutase (SOD)-like activity measured by the NBT reduction method or xanthine–xanthine oxidase assay further indicated that the complex mimics metalloenzyme behavior, exhibiting higher percentage inhibition of formazan formation relative to the ligand. In summary, the combined spectroscopic, mass, diffraction, and biological studies clearly demonstrate that the Schiff-base ligand and its Zn(II) complex are successfully synthesized and structurally validated. The Zn(II) complex exhibits superior antimicrobial, antioxidant and SOD-mimetic, highlighting its potential as a multifunctional bioactive coordination compound. This study provides a solid foundation for further exploration of antipyrine-derived Schiff base metal complexes in biomedical and pharmaceutical applications.

## References

- [1] Yimer A M, et al. Spectromagnetic and antimicrobial studies on some 3d metal complexes with ethylenedianil of ortho-hydroxyphenylglyoxal. *Am J Appl Chem*, 2014; 2:8-15.
- [2] Klein A V and Hambley TW. Platinum drug distribution in cancer cells and tumors *Chem. Rev.*, vol.2009; 109(10):4911-4920.
- [3] Gust R, Beck W, Jaouen G and Schonenberger H. Optimization of cisplatin for the treatment of hormone dependent tumoral diseases Part 1: use of steroidal ligands. *Coord. Chem. Rev.*, 2009; 253(21):2742-2759.
- [4] Malhotra E, Kaushik NK and Malhotra HS. Synthesis and studies of ionic chelates of hafnocene with guanine. *Indian J Chem*, 2006; 45(2):370-376.
- [5] Chandra S, Shukla D, Gupta LK. Synthesis and spectroscopic studies of Co(II), Ni(II) and Cu(II) complexes with N donor (N4) macrocyclic ligand (DSLFF). *J Indian Chem Soc.*, 2006; 85:800-806.
- [6] S. Syed Ali Fathima, M. Mohamed Sahul Meeran, E. R. Nagarajan *Journal of Molecular Liquids*, 2791 (2019) 177-189.
- [7] K. Nagashri, "Synthesis characterization and pharmacological studies of copper complexes derived from flavone derivatives", Ph.D. dissertation, Dept. Chem., Noorul Islam Univ., Tamilnadu, 2013.
- [8] Raja JD, Sakthikumar K. Synthesis of water soluble transition metal(II) complexes from morpholine condensed tridentate Schiff base: structural elucidation, antimicrobial, antioxidant and DNA interaction studies. *J Chem Pharm Res.*, 2015; 7:23-34.
- [9] N. Jyothi, Nirmala Ganji, Sreenu Daravath, Shivaraj, *Journal of Molecular Structure*, 12075 (2020) 127799.
- [10] Azza A. Hassoon, Roger G. Harrison, Nagwa Nawar, Stacey J. Smith, Mohsen M. Mostafa, *Journal of Molecular Structure* Volume 12035 March 2020 Article 127240.
- [11] Raman N, et al., Novel metal based pharmacologically dynamic agents of transition metal(II) complexes: designing, synthesis, structural elucidation, DNA binding and photo-induced DNA cleavage activity. *Spectrochim Acta A Mol Biomol Spectrosc.*, 2010; 75:88-97.
- [12] Muhammad Iqbal, Amir Karim, Saqib Ali, Muhammad Nawaz Tahir, Manzar Sohail, *Polyhedron* Volume 1781 March 2020 Article 114310.
- [13] Bheemarasetti M, et al., Novel Schiff base metal complexes: synthesis, characterization, DNA binding, DNA cleavage and molecular docking studies, *Journal of the Iranian Chemical Society*, 2018; 15(6):1377-1389.
- [14] Barış Kurt, Hamdi Temel, Metin Atlan, Savaş Kaya, *Journal of Molecular Structure* Volume 12095 June 2020 Article 127928.
- [15] Tan C, et al., Synthesis, structural characteristics, DNA binding properties and cytotoxicity studies of a series of Ru(III) complexes, *J Inorg Biochem.*, 2008; 102: 1644-1653.
- [16] Muhammad S, Nooruddin, et al., Synthesis, spectroscopic characterization, crystal structure, DNA interaction study and in vitro biological screenings of 4-(5-chloro-2-hydroxyphenylamino)-4-oxobut-2-enoic acid, *Spectrochim Acta A: Mol and Biomol Spectrosc.*, 2015; 134:244-250.
- [17] Babahan, I., Eydurán, F., et al., Spectroscopic and biological approach of Ni(II), Cu(II) and Co(II) complexes of 4-methoxy/ethoxybenzaldehyde thiosemicarbazone glyoxime,

- Spectrochimica Acta Part A: Molecular and Biomolecular Spectroscopy*, 2014; 121:205–215.
- [18] Tyagi, P., Tyagi, M., et al., Synthesis, characterization of 1,2,4-triazole Schiff base derived 3d-metal complexes: Induces cytotoxicity in HepG2, MCF-7 cell line, BSA binding fluorescence and DFT study, *Spectrochimica Acta Part A: Molecular and Biomolecular Spectroscopy*, 2017; 171:246–257.
- [19] N. Raman, S. J. Raja, et al., Designing, structural elucidation, comparison of DNA cleavage and antibacterial activity of metal (II) complexes containing tetradentate Schiff base, *Russ. J. Coord. Chem.*, 2008; 34:842-848.
- [20] Raman N, Sakthivel A, Rajasekaran K, Design, structural elucidation, DNA interaction and antimicrobial activities of metal complexes containing tetraazamacrocyclic Schiff bases, *J. Coord. Chem.*, 2009; 62:1661-1676.
- [21] P. Uma Maheswari, V. Rajendiran, et al., Mixed ligand Ruthenium(II) complexes of 5,6-dimethyl-1,10 phenanthroline: The role of ligand hydrophobicity on DNA binding of the complexes, *Inorg. Chem. Acta*, 2006; 359(14):4601-4612.
- [22] Aazam ES, El Husseiny AF, Al-Amri HM, Synthesis and photoluminescent properties of a Schiff-base ligand and its mononuclear Zn(II), Cd(II), Cu(II), Ni(II) and Pd(II) metal complexes, *Arab J Chem.*, 2012; 5:45-53.
- [23] Ramman N., Raja Y. P. and Kulandaisory A, Synthesis and characterization Cu(II), Ni(II), Mn(II), Zn(II), and Vo(II) Schiff base complexes derived from o-phenylenediamine and acetoacetanilide, *Indian Academy of Science*, 2001; 113(3):183-189.
- [24] Williams D. H. and Fleming I., *Spectroscopic Methods in organic Chemistry*, Mc. Graw Hill, London. Springer international publishing, 2019
- [25] Marialena Lazou, Alketa Tarushi, Panagiotis Gritzapis, George Psomas, *Journal of Inorganic Biochemistry*, 206 (2020) 111019.
- [26] Anindita De, Hari Prakash Ray, Preeti Jain, Harsimrut Kaur, Nikita Singh, *Journal of Molecular Structure*, 11995 (2020) 126901.
- [27] Ayşin Zülfikaroğlu, Çiğdem Yüksektepe Ataoğlu, Emine Çelikoğlu, Umut Çelikoğlu, Önder İdil, *Journal of Molecular Structure*, 11995 (2020) 127012
- [28] S.-H. Hsieh, Y.-P. Kuo, H.-M. Gau, Synthesis, characterization, and structures of oxovanadium (V) complexes of Schiff bases of  $\beta$ -amino alcohols as tunable catalysts for the asymmetric oxidation of organic sulfides and asymmetric alkynylation of aldehydes, *Dalton Trans.*, 2007; 1(1):97–106.
- [29] Uma V, Kanthimathi M, et al., Oxidative DNA cleavage mediated by a new copper(II) terpyridine complex: crystal structure and DNA binding studies. *J. Inorg. Biochem.*, 2005; 99(12):2299-2307.
- [30] Sakthikumar et al., Antimicrobial, Antioxidant and DNA Interaction Studies of Water-soluble Complexes of Schiff Base Bearing Morpholine Moiety, *Indian J. Pharm.Sci.*, 2018; 80(4):727-738.